

Clutter-suppressing performance estimation methods of active sonar waveform based on reverberation statistical models in littoral environment

Chi Zhang¹, Xiaochuan Ma¹✉, Yongqing Wu¹, Li Jiang¹, Fei Zhan¹, Shuhao Zhang¹

¹Key Laboratory of Information Technology for Autonomous Underwater Vehicles, Institute of Acoustics, Chinese Academy of Sciences, Beijing 100190, People's Republic of China

✉ E-mail: maxc@mail.ioa.ac.cn

Abstract: Detecting low-speed quiet targets such as divers and underwater-unmanned-vehicles in littoral environment by using active sonar is becoming increasingly attractive. When using a Doppler insensitive pulsed linearly frequency modulated signal, the high-level clutters which might arise from underwater physical scatterers will lead to excessive false alarm rates and limit the detection performance. However, Doppler sensitive waveforms such as binary phase shift keying have the capability of filtering clutters and degrading false alarms. Thus, the question how to estimate the clutter-suppressing performance of waveforms is essential for sonar system design. In this study, the clutter-rejecting principle of waveform is theoretically introduced firstly. Then, based on the reverberation statistical features, this study proposes two methods, the Doppler-statistic method and envelope-statistic method, separately, to estimate and evaluate the clutter suppressing performance of waveforms. Finally, the methods are verified by lake experiments. It is proved that the first method has the capacity of calculating the confidence probability of suppressing clutters by a waveform, and through the second method, the clutter rejecting performance of waveforms can be evaluated and verified. The methods can be used for selecting and designing waveforms to reduce false alarms and improve detection performance.

1 Introduction

1.1 Motivation

Currently, the detection of harbour low-speed quiet intruders such as underwater-unmanned-vehicles (UUVs) and divers is highly required. The active sonar is regarded as an appropriate choice, but the echoes of low-Doppler targets are always blended with high-level discrete clutters when we use linearly frequency modulated (LFM) waveform in shallow water, which heavily increases the probability of false alarm (P_{fa}). The experiment results indicate that Doppler sensitive waveform performs better in reducing clutters and decreasing P_{fa} than insensitive one in low-speed target detection, which is termed as ‘clutter filter’ effect [1, 2]. By comparison, it seems that sensitive waveforms are more suitable to be used on high-frequency sonar for short range detection, because the distortion of a long pulse may result in energy loss of matched filtering. The exact estimation of waveform clutter rejecting performance is important for waveform selection and design. The traditional methods of evaluating waveform performance always focus on waveform types and parameters. For instance, smaller Doppler tolerance may indicate better clutter rejecting ability of waveform. However, as clutters are closely bound up with environmental factors, the traditional methods do not take into account any environmental conditions. So it cannot be simply used to estimate the waveform clutter suppressing performance since it cannot reflect the clutters changes. The authors are motivated to find more efficient methods.

For the reason that clutters and environmental information are embodied in reverberation, the authors are enlightened to develop two methods based on the statistical analysis of reverberation data. Based on the reverberation Doppler spread statistical model, we propose the first Doppler-statistic method to estimate the clutter suppressing probability of a waveform. It relies on the measurement of reverberation channel Doppler dispersion function. Then we propose the second envelope-statistic method to evaluate and compare the clutter suppressing ability of waveforms according to the variation of statistical parameters of reverberation

envelope. Both the two methods employ the statistical features of reverberation, and could be realised by statistical analysis of reverberation data. It is proved by experiments that both methods are effective and feasible. Moreover, the methods are useful for active sonar waveform selecting and designing.

1.2 Literature

Clutter is regarded as part of reverberation in this paper. We redeclare the concept of reverberation and clutter in this section according to the physical and statistical mechanisms. Then we introduce the research progress of reverberation Doppler dispersion and reverberation envelope statistical models.

1.2.1 Clutter: Reverberation is the summation of backscattering echoes from scatterers distributed in water surface, seafloor and water volume. As shown in [1, 3, 4], clutters could be defined as a high-level target-like output after beamforming and matched filtering, which might arise from large scatterers such as rocks, shipwrecks, seaweeds, fishes and mountains and lead to the formation of false alarms. Commonly speaking, the velocity of scatterers is usually small or nearly zero. Thus, it is confusing and always leading to false alarms when target speed is also quite small. Similar with the analysis in [3, 4], this paper treats clutter as a component of reverberation, which will change the reverberation characters. Except for the clutter, interference is another factor which increases false alarms. The reason for the interference formation is that the number of scatterers in a resolution cell may not be large enough to satisfy the central limit theorem (CLT), hence the envelope distribution may deviate from Rayleigh model to a heavy-tailed non-Rayleigh distribution [5]. The two factors causing false alarms are totally different. Clutter factor is formed by false targets, and it is more consistent over frequency. Interference factor is formed by random summation of amplitudes, and it is less consistent over frequency [3]. Clutter is a stationary physical false alarm, while interference is a statistical false alarm

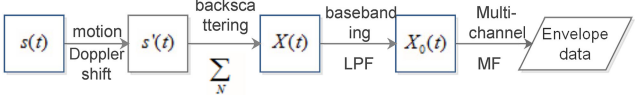


Fig. 1 Block diagram of receiver signal model

and not stationary between ping-to-ping. In this paper, only the problem of how to reduce clutters is taken into consideration.

1.2.2 Reverberation Doppler dispersion: Under the assumption of wide-sense stationary uncorrelated scattering, as scatterers are independent with each other, the Doppler spread of reverberation channel can be described as the Doppler dispersion function. The Doppler spread of reverberation mainly arises from scatterers motion, for instance, air bubbles, marine organisms and moving interfaces (sea surface in the presence of waves). When sonar platform is moving, the multipath effect can also result in Doppler spread [6]. As clutters are parts of reverberation, high-level clutters may be distributed in larger Doppler range as a result of Doppler spread phenomenon. Thus, the severity of reverberation Doppler spread has great influence on low-speed target detection. Researchers found that the dispersion function could be described by statistical models, such as Gaussian distribution, two-side exponential distribution and so on [7]. Due to the fact that the Doppler spread of clutters and reverberation are independent identically distributed, we can use the statistical model to represent the Doppler spread of clutters. The dispersion function and Doppler spread statistical model could be measured and estimated through experiments, respectively. In this paper, it is proposed to calculate clutter suppressing confidence probability of a waveform by using the statistical model.

1.2.3 Reverberation envelope statistical models: As mentioned above, clutter and interference are the main factors leading to the departure of reverberation envelope statistics from traditional Rayleigh model to a heavier-tailed distribution. Much attention has been put on non-Rayleigh reverberation in recent years with the development of high-resolution active sonar system. In the earlier studies, many statistical models such as log-normal, Weibull, *K* and mixture distributions are presented to well fit the heavy-tailed envelope [4, 5, 8, 9]. In particular, Abraham and Lyons [5] proposed the relationship between environmental parameters and *K*-distribution (KD) model. The sonar system and environment are the two main factors resulting in the variation of KD parameters. Although some works focusing on the relationship between sonar parameters and the statistical models have been done, few works are mentioned concerning the waveform influence on reverberation statistics [10, 11].

1.3 Description of paper

This paper proposes two methods on estimating the clutter-suppressing performance of waveforms based on reverberation statistical characters. The methods are helpful for sonar designers to select and design waveform for filtering clutters and improving the performance of detecting low-speed targets. Through Doppler-statistic method, we can achieve the clutter suppressing probability of waveforms according to reverberation Doppler spread statistical model. With the envelope-statistic method, the clutter suppressing ability of waveforms can be evaluated and compared on the basis of reverberation envelope statistical model.

The paper is organised as follows. In Section 2, the principle of clutter rejecting is explained theoretically. Section 3 details the proposed two methods. Section 4 conducts real data analysis to verify the methods above. In Section 5, conclusion is presented.

2 Modelling

On the basis of point scattering theory, this section introduces reverberation model including background reverberation and clutters. Multi-channel matched filter (MF) is processed on received data. Then the Doppler spread statistical model and the envelope statistical model adopted in this paper are introduced in

details. Furthermore, we take LFM and BPSK waveforms as examples to illustrate the clutter rejecting principle of waveforms.

2.1 Receiver model

The point scattering model is widely used in reverberation simulation especially on high-frequency active sonar [12]. Data received by sonar come of the backscattering echoes from underwater scatterers. In this paper, we adopt narrow band condition because the relative bandwidth is small and the narrow-band hypotheses are satisfied [13–15]. The signal model of receiver is generalised in Fig. 1.

Assuming the transmitted pulse is given by

$$s(t) = u(t) \cdot e^{j2\pi d_c t}, \quad (1)$$

where $u(t)$ is the baseband signal and d_c is the Doppler shift derived from carrier frequency f_c . Accounting for the motion velocity v_x of sonar platform, the Doppler shift by platform motion is approximately

$$d_x = \frac{2v_x}{c} d_c \cos\theta, \quad (2)$$

where c is the velocity of underwater sound and θ is the transmitting angle relative to sonar motion direction. Define

$$s'(t) = u(t) \cdot e^{j2\pi d_0 t}, \quad (3)$$

where $d_0 = d_c + d_x$. Hence, the response of each scatter is modelled as a time-delayed and amplitude-scaled version of $s'(t)$. The received data can be described as

$$\begin{aligned} X(t) &= As'(t - \tau_i)e^{j2\pi\Delta d_i t} + \sum_{i=1}^{N-M} B_i s'(t - \tau_i)e^{j2\pi\Delta d_i t} \\ &\quad + \sum_{j=1}^M C_j s'(t - \tau_j)e^{j2\pi\Delta d_j t} + V(t) \\ &= Au(t - \tau_i)e^{j2\pi(d_0 + \Delta d_i)t} + \sum_{i=1}^{N-M} B_i u(t - \tau_i)e^{j2\pi(d_0 + \Delta d_i)t} \\ &\quad + \sum_{j=1}^M C_j u(t - \tau_j)e^{j2\pi(d_0 + \Delta d_j)t} + V(t), \end{aligned} \quad (4)$$

where $V(t)$ is the ambient noise, A , B_i , C_j and τ_i , τ_i and τ_j are the amplitudes and time delays of target echo, background scatterers and clutters, respectively. Δd_i is the Doppler shift derived by target velocity, Δd_i and Δd_j are Doppler shifts of each scatter and clutter. Reverberation is modelled as backscattering summation of N scatterers including M distinct high-level clutters with large amplitude. The baseband signal $X_0(t)$ can be obtained by frequency shifting and low-pass filtering

$$\begin{aligned} X_0(t) &= \text{LPF}\{X(t)e^{-j2\pi d_0 t}\} \\ &= Au(t - \tau_i)e^{j2\pi\Delta d_i t} + \sum_{i=1}^{N-M} B_i u(t - \tau_i)e^{j2\pi\Delta d_i t} \\ &\quad + \sum_{j=1}^M C_j u(t - \tau_j)e^{j2\pi\Delta d_j t} + V_0(t) \\ &= T(t) + B(t) + C(t) + V_0(t), \end{aligned} \quad (5)$$

where $\text{LPF}\{\cdot\}$ represents the low-pass filtering operation. $V_0(t)$ is the ambient noise after low-pass filtering. Matched filtering is adopted to process the received data, while the target item $T(t)$ and clutter item $C(t)$ are well correlated with the transmitted signal and might be highlighted by MF process. The well-known Woodward ambiguity function (WAF) of $u(t)$ is defined as $\chi_u(\tau, d)$ under narrow-band hypothesis [14]. After being matched filtered by a

replica of Doppler shift d , the target and clutter items $T(t)$ and $C(t)$ could be described as

$$\begin{aligned} R_{ut}(\tau, d) &= \int u(t)T^*(t + \tau_t)e^{j2\pi dt}dt \\ &= A \int u(t)u^*(t + \tau_t)e^{j2\pi(d - \Delta d_t)t}dt \\ &= A \int U^*(f)U(f - (d - \Delta d_t))e^{-j2\pi f \tau_t}df \\ &= A \chi_u(\tau_t, d - \Delta d_t), \end{aligned} \quad (6)$$

and

$$\begin{aligned} R_{uc}(\tau, d) &= \int u(t)C^*(t + \tau)e^{j2\pi dt}dt \\ &= \int u(t) \left(\sum_{j=1}^M C_j u^*(t + \tau_j) e^{j2\pi(d - \Delta d_j)t} \right) e^{j2\pi dt} dt \\ &= \sum_{j=1}^M C_j \int U^*(f)U(f - (d - \Delta d_j))e^{-j2\pi f \tau_j}df \\ &= \sum_{j=1}^M C_j \chi_u(\tau_j, d - \Delta d_j). \end{aligned} \quad (7)$$

When $d = \Delta d_t$, R_{ut} will be the maximum value at time delay τ_t , and R_{uc} will be decided by $\chi_u(\tau_j, \Delta d_t - \Delta d_j)$ whose value depends on waveform WAF χ_u , clutter Doppler shift Δd_j and target speed Δd_t . The Doppler shifts of M clutters are not equal, and it cannot be decided simply by the j th value Δd_j or the average value $(1/M)\sum \Delta d_j$. Since clutters are parts of reverberation, the Doppler spread of clutters will follow the reverberation model if reverberation Doppler spread could be described by a statistical model. In other words, Δd_j will follow the distribution. In this paper, we apply the statistical model of clutters Doppler shifts on analysing the clutter reducing problem.

2.2 Statistical model of reverberation Doppler spread

As Δd_j is the Doppler deviation of the j th clutter, it is assumed that Δd_j follows a statistical model with probability density function (PDF) $p(\Delta d_j)$. Murray [7] proposed that scatterers Doppler spread distribution could be approximately described as a two-side exponential distribution according to the empirical sea test data analysis, the PDF is

$$p(\Delta d_j) = \frac{\mu}{2} e^{-\mu|\Delta d_j|}, \quad (8)$$

where μ is a parameter representing the Doppler spread slope s , which is ranging between 6 and 20 dB/knot from a variety of sea tests. Equation (8) is commonly interpreted as an environmental Doppler spreading function. μ could be solved based on the definition of s from equation

$$20\log_{10} \left[\frac{p(0)}{p(1)} \right] = s(\text{dB}), \quad (9)$$

then

$$\mu = \ln(10^{(s/20)}). \quad (10)$$

In this paper, this model is adopted to describe the Doppler spread because it bears explicit physical meaning and has been proved through experiments. The calculation of waveform clutter suppressing probability will be derived based on the model in Section 3.1.

2.3 Statistical model of reverberation envelope

The envelope and instantaneous intensity of the MF output are often used to form detectors because they are sufficient statistics for detection, including Rayleigh distribution and non-Rayleigh with a circularly symmetric complex envelope pdf such as KD [5]. As clutters lead to heavier-tailed non-Rayleigh distribution of reverberation envelope statistics, the statistical parameters can be applied to evaluate the waveform clutter reducing problem. The amplitude B_i of $(N-M)$ scatterers follows Gaussian distribution and its envelope follows Rayleigh distribution as scatterers number $(N-M) \rightarrow \infty$. If not, it will deviate from Rayleigh distribution because CLT is not satisfied [5]. The number of clutters M is small but the amplitude C_j is big, which contributes to the heavy tails and leads to non-Rayleigh reverberation. Besides the fact that KD fits well on experimental data, KD has clear physical interpretation of its two parameters: shape parameter α and scale parameter λ [5]. The parameters should be estimated from a finite sample of independent and identically distributed MF-envelope data. The number of data is typically between several hundred and one thousand at least [16]. This paper adopts KD to describe the heavy-tailed reverberation envelope data. The PDF and cumulative distribution function (CDF) of KD for the reverberation MF envelope are, respectively,

$$p_K(y) = \frac{4}{\sqrt{\lambda}\Gamma(\alpha)} \left(\frac{y}{\sqrt{\lambda}} \right)^\alpha K_{\alpha-1} \left(\frac{2y}{\sqrt{\lambda}} \right), \quad (11)$$

and

$$F_K(y) = 1 - \frac{2}{\Gamma(\alpha)} \left(\frac{y}{\sqrt{\lambda}} \right)^\alpha K_\alpha \left(\frac{2y}{\sqrt{\lambda}} \right), \quad (12)$$

where α and λ are the shape and scale parameters, respectively, $K_v(z)$ is the Basset function (i.e. a modified Bessel function of the third kind). The intensity is $E[Y^2] = \alpha\lambda$. α and λ represent the deviation tendency from Rayleigh distribution and the reverberation intensity, respectively. As $\alpha \rightarrow \infty$ KD turns to be Rayleigh distribution. The smaller α means heavier-tailed and higher false alarm rates, i.e. α could be an indicator pointing to the P_{fa} prediction [17].

2.4 Waveforms

As mentioned earlier, the classical FM waveform is often selected for low-speed target detection, but the existence of clutters brings more false alarms. However, the Doppler sensitive BPSK waveform is experimentally proved efficient for reducing clutters. Recently, due to BPSK's ideal ambiguity function shaped as a thumbtack with both high Doppler and range resolution [18, 19], a growing number of works take BPSK as a detection waveform on active sonar system. For the sonar system with limited bandwidth, we always hope that the bandwidth and time-duration product (BT) of waveform should be as large as possible to increase the signal processing gain. The larger BT is, the smaller Doppler tolerance of BPSK will become, while the larger Doppler tolerance of LFM will be. BPSK has the same BT value with LFM but better clutter rejecting performance. Thus, we choose LFM and BPSK of the same B , T and frequency as compared to analyse the methods proposed in this paper. LFM and BPSK waveform could be expressed as

$$S_{\text{lfm}}(t) = \sin(2\pi f_c t + \pi k t^2), \quad t \in [0, T], \quad (13)$$

and

$$S_{\text{bpsk}}(t) = \sin[2\pi f_c t(2b(t) - 1)], \quad t \in [0, T]. \quad (14)$$

where f_c is the carrier frequency, $k = (B/T)$ is the frequency modulation factor of LFM, and $b(t)$ is a binary sequence of N bits [2]. It is proved in [20] that m -sequence coded BPSK has good

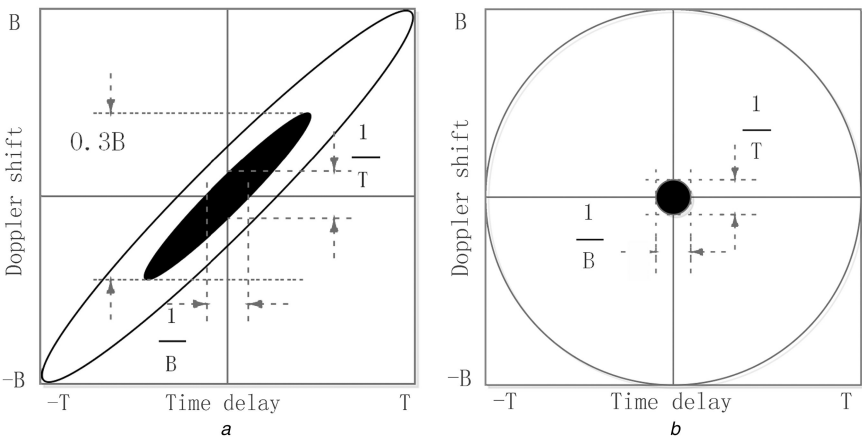


Fig. 2 Ambiguity function contour of LFM and BPSK waveforms, the black area is the region of -3 dB contour
(a) LFM, (b) BPSK

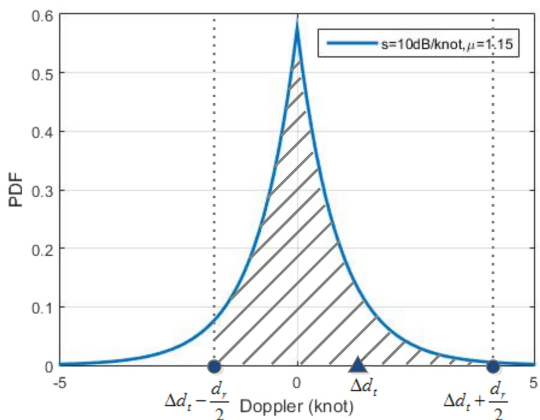


Fig. 3 Doppler spread statistical model and MF process of clutters

cross-correlation properties and minimal inter-sequence interference. The 3-dB bandwidth of BPSK is

$$B = \frac{N}{T}, \quad (15)$$

where $N = BT$ is the BT product. BPSK is able to control BT easily by changing N . The WAF sections of LFM and BPSK are shown in Fig. 2. The definition of -3 dB Doppler tolerance d_r is that

$$\chi_u(\tau, d_r) = \frac{\sqrt{2}\chi_u(0, 0)}{2}. \quad (16)$$

The sidelobe level (SLL) of BPSK [2] is

$$\text{SLL} = -10\log_{10}(N), \quad (17)$$

$\text{SLL} < -3$ dB as $N > 2$. So the sidelobe has no influence on the Doppler tolerance as BT is large enough in this paper. It can be found that LFM and BPSK which have the same Doppler and range resolution have different Doppler tolerance d_r . The Doppler tolerance of LFM may be estimated as $d_r \approx 0.3B$ which is normally much bigger than $d_r \approx (1/T)$ of BPSK when $BT \gg 1$ in most cases. When Δd_j of (7) matching on the black region in Fig. 2, the value of $R_{uc}(\tau, d)$ is quite large and may exceed the given threshold being an undesired clutter. BPSK is easier to mismatch the black region than LFM which means BPSK is a Doppler sensitive waveform. This may lead to the result that clutters will be more easily missed by BPSK if Δd_j mismatches the black region.

3 Proposed two methods

The above section illustrates that the Doppler sensitivity of waveform is the key point of rejecting clutters. However, clutter reducing performance estimation is closely related with the severity of reverberation Doppler spread, and the existence of clutters will lead to variation of the statistical parameters of envelope data. Based on statistical models of reverberation Doppler spread and envelope data, this section introduces two novel methods, Doppler-statistic method and envelope-statistic method, respectively.

3.1 Doppler-statistic method: based on reverberation Doppler spread model

When the Doppler shift of replica is $d = \Delta d_t$, and the Doppler tolerance of waveform is d_r , the relationship between waveform and Doppler spread model of clutters is simulated in Fig. 3. It is assumed that $s = 10$ dB/knot, and then $\mu = 1.1513$. It is shown that there will be high-level clutters in Doppler range $[\Delta d_t - (d_r/2), \Delta d_t + (d_r/2)]$, where $d_r > 0$, and the clutters outside will be rejected by the waveform. Thus, the clutter suppressing confidence probability of a waveform can be defined as

$$p_I = \int_{-\infty}^{\Delta d_t - (d_r/2)} p(\Delta d_j) d\Delta d_j + \int_{\Delta d_t + (d_r/2)}^{+\infty} p(\Delta d_j) d\Delta d_j, \quad (18)$$

where $0 < p_I < 1$. On the basis of the equation, we can calculate the clutter suppressing probability when we employ a waveform with Doppler tolerance d_r to detect a target of velocity Δd_t . From (18), the larger $|\Delta d_t|$ and smaller d_r , the bigger probability of rejecting clutters. It means that clutters have little impact on detection performance when target speed is high enough. Moreover, the more Doppler sensitive waveform is, the better the clutter reduction capacity will be. Substituting (18) into (8)

$$p_I = \begin{cases} \frac{1}{2}e^{\mu(\Delta d_t - (d_r/2))}[1 - e^{\mu d_r}] + 1, & \Delta d_t \leq -\frac{d_r}{2}; \\ \frac{1}{2}e^{\mu(\Delta d_t - (d_r/2))}[1 + e^{-2\mu\Delta d_t}], & -\frac{d_r}{2} < \Delta d_t \leq \frac{d_r}{2}; \\ -\frac{1}{2}e^{-\mu(\Delta d_t - (d_r/2))}[1 - e^{-\mu d_r}] + 1, & \Delta d_t > \frac{d_r}{2}. \end{cases} \quad (19)$$

Thus, the clutter suppressing probability could be calculated according to waveform Doppler tolerance and reverberation Doppler spread statistical model. For example, as shown in Fig. 3, when $\Delta d_t = 1$ kt, $d_r = 6$ kt, then $p_I = 0.055$. In this case, few clutters can be rejected and most of them will become false alarms. If d_r decreases to 1 kt, p_I will increase to 97.77% to reject almost all clutters. Hence, we can predict that BPSK has much higher probability of rejecting clutters than LFM.

Furthermore, concerning sonar design, if a minimum confidence probability p_I is required where $0 < p_I < 1$, the

maximum value of d_r can be derived from (18). For two-side exponential model, it can be calculated from (19) that

$$d_r = \begin{cases} \frac{2}{\mu} \ln \left[\sqrt{\frac{(p_I - 1)^2}{e^{2\mu\Delta d_t}} + 1} - \frac{p_I - 1}{e^{\mu\Delta d_t}} \right], & \Delta d_t \leq -\frac{d_r}{2}; \\ -\frac{2}{\mu} \ln \left[\frac{2p_I}{e^{\mu\Delta d_t} + e^{-\mu\Delta d_t}} \right], & -\frac{d_r}{2} < \Delta d_t \leq \frac{d_r}{2}; \\ \frac{2}{\mu} \ln \left[\sqrt{\frac{(p_I - 1)^2}{e^{-2\mu\Delta d_t}} + 1} - \frac{p_I - 1}{e^{-\mu\Delta d_t}} \right], & \Delta d_t > \frac{d_r}{2}. \end{cases} \quad (20)$$

Then we can achieve the range of Δd_t value from the corresponding expression of d_r . However, it is hard to solve the high-order inequality of (20) and the complex solution is not practical for engineering. Thus, an approximation method is needed to replace it.

Generally, the environmental Doppler spread is not quite serious. Even when $s = 6$ dB/knot which is regarded as the most serious situation described in [7], derived from (8) and (10), 95% spreads will distribute in a small range [-4.33, 4.33] kt. However, the target speed of a typical diver of UUVs is about 1 to 4 kn and the Doppler tolerance of a waveform cannot be too small because the pulse duration cannot be so long especially on high-frequency active sonar system. According to Fig. 3, the cumulative probability of negative Doppler range will dominate the value of p_I when $\Delta d_t > 0$. Then the second expression of (18) can be neglected, and the estimation of p_I will be more conservative. Moreover, Equation (18) can be approximated as

$$p_I \approx \begin{cases} \int_{-\infty}^{I_+} p(\Delta d_j) d\Delta d_j, & \Delta d_t > 0; \\ \int_{I_-}^{+\infty} p(\Delta d_j) d\Delta d_j, & \Delta d_t < 0. \end{cases} \quad (21)$$

where $I_+ = \Delta d_t - (d_r/2)$ as $\Delta d_t > 0$ and $I_- = \Delta d_t + (d_r/2)$ as $\Delta d_t < 0$. Typically, the given p_I is much larger than 50%, then $I_+ > 0$ and $I_- < 0$ are required. Based on Fig. 3, if

$$\begin{cases} \Delta d_t - \frac{d_r}{2} > I_+, & \Delta d_t > 0; \\ \Delta d_t + \frac{d_r}{2} < I_-, & \Delta d_t < 0. \end{cases} \quad (22)$$

satisfied, the clutter suppressing probability will be larger than given p_I . If the statistical model is assumed symmetry such as two-side exponential distribution, (22) can be summarised by

$$|\Delta d_t| > \frac{d_r}{2} + I, \quad (23)$$

where $I = I_+ = -I_- > 0$ is named as the confidence interval. According to (8) and (21), the I of two-side exponential model is

$$I = -\frac{\ln[2(1 - p_I)]}{\mu}. \quad (24)$$

For instance, as $\mu = 1$, $p_I = 0.95$, then $I = 2.30$ which means that if

$$|\Delta d_t| - \frac{d_r}{2} > 2.3 \text{ kt}, \quad (25)$$

the clutter rejecting probability will be larger than 95%.

In this Doppler-statistic method, we can measure the parameter μ of Doppler spread statistical model by experiments. Commonly, the Doppler spread function of reverberation could be measured by a very long sinusoid transmission. The longer pulse, the higher precision. For example, 1 s long sinusoid pulse corresponding to Doppler precision of 1 Hz. Typically, we can transmit repeated

pulses and normalise sampled data to stabilise the reverberation data firstly. For instance, the split-window normalisation method could be used here [1]. After normalisation, we can process the data by short-time Fourier transform. Then, the statistical reverberation spectrum can be calculated by averaging. After that, we can get the optimal fitting parameter $\hat{\mu}$ of the two-side exponential model from the spectrum. Thus, clutter suppressing probability can be derived based on the model with parameter $\hat{\mu}$.

Based on the measurement of reverberation channel, Doppler-statistic method could help sonar designer to estimate the waveform clutter rejecting ability statistically. It is beneficial to choose waveform and design parameters. It should be noted that there are many different methods of measuring reverberation Doppler spread, which will determine the accuracy of measurement and calculation.

3.2 Envelope-statistic method: based on reverberation envelope statistical model

The quantity of clutters will lead to variation of envelope statistics. For KD model, the shape parameter α could be an indicator to the clutters. The basebanded envelope data should be decimated firstly so that the sampling frequency is equal to the bandwidth [10]. Similar with Doppler-statistic method, data should be normalised to stabilise the reverberation. Then we can use algorithms such as Bayesian-based method-of-moments to estimate KD parameters [16]. Furthermore, the estimation results have to pass the Kolmogorov-Smirnov (KS) test [9] to verify that the envelope data are well fitted by KD. After these procedures, we may get credible and consistent results in different experiments. According to the above analysis, false alarms in littoral environment are mainly caused by clutters, and α can indicate the probability of false alarm. Hence, the estimated $\hat{\alpha}$ can be used to evaluate the clutter suppressing performance of waveforms as follows:

- If $\hat{\alpha} \rightarrow \infty$ (typically when $\hat{\alpha} > 20$), it represents that no clutters left and puts on good clutter rejecting performance of the waveform.
- Smaller $\hat{\alpha}$ indicates larger quantity of existing clutters and worse clutter rejecting performance.
- If $\hat{\alpha}$ maintains constant and fails to reach infinity as the Doppler shift of MF replica $|d|$ increases, it means that further waveform changes will not improve the heavy-tail performances. Moreover, there are limitations on clutter rejection improvement by waveform. The clutters which cannot be rejected by waveform might be the statistical interference referred in Section 1.

Although a detailed clutter suppressing probability cannot be obtained here, the envelope-statistic method effectively verifies and compares the clutter rejecting performance by the estimation and comparison of $\hat{\alpha}$. Particularly speaking, non-extra experiments are needed in this method, and it is easily realised through received data. In the application of constant false alarm rate detection, the estimation of statistical model is necessary. The proposed method means that the statistical parameters can not only be used to design threshold, but also to quantify the clutters in reverberation. For the purpose of varying environments on a moving platform especially, the $\hat{\alpha}$ of each pulse guarantees the stable clutter rejecting performance through conducting feed-back to update the waveform. According to the above analysis, the $\hat{\alpha}$ of BPSK reverberation envelope should be obviously larger than LFM.

The two methods proposed above, Doppler-statistic method and envelope-statistic method, are both on the basis of statistic theory. The Doppler-statistic method needs to measure the reverberation channel Doppler spread, while the envelope-statistic method needs to estimate the parameters of reverberation envelope data. Even though the measurement and estimation methods are not the key point of this paper, they are quite essential for the realisation and application of the two methods. The measurement and estimation procedures should be normalised to get consistent results during separate experiments. If the two-side exponential model and KD

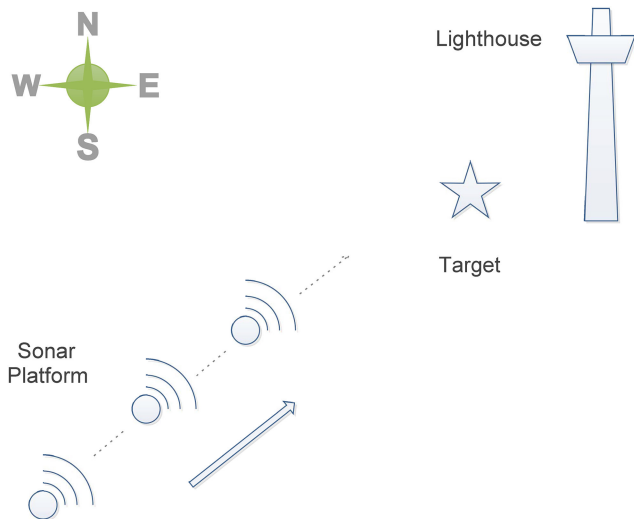


Fig. 4 Experiment scenario: sonar platform moving towards a low-speed target and lighthouse which in the same direction

model are not well fitted, we could process a similar analysis using other proper statistical models.

4 Experiment

The waveform clutter-suppressing principle is introduced in Section 2. It is declared that Doppler sensitive waveform has larger probability to reject clutters than Doppler insensitive waveform. Based on two-side exponential model and KD model, in Section 3, two statistical methods are proposed to estimate the clutter suppressing ability of waveforms. In this section, we performed low-speed target detection experiments using LFM and BPSK and given data analysis to verify the two proposed methods.

4.1 Experiment description

Experiments are conducted in a man-made filled lake with underwater mounds and complex geographic characteristics. The water depth is <75 m in the region where the experiments were carried out. It seems to be a typical shallow water environment just like the harbour or littoral environment. The lake trial was held in 2015, and several experiments are focused on BPSK waveform detection performance on a high-frequency sonar platform. By comparison, we also took LFM waveform experiments with the same bandwidth, time duration and frequency. A target is set at a distance about 2 km from the original sonar location with a velocity of about 1 kn towards the sonar. About 300 m away from the target, there is a lighthouse standing on the seafloor which might be a strong clutter source. The sonar platform transmits ping-to-ping and moves towards the target and lighthouse direction. The experiment scenario is described in Fig. 4.

4.2 Data analysis

According to Doppler-statistic method in Section 3.1, the authors measured the reverberation Doppler dispersion function and estimated the parameter $\hat{\mu}$ of two-side exponential distribution. The process of measurement is not detailed here. The result is that $\hat{\mu} = 6$, substitute to (10) then $s = 52 \text{ dB/kt}$ which represents quite slight Doppler spread. The lake environment with little Doppler dispersion is quite favourable. In our experiments, the bandwidth and time duration of LFM and BPSK are both 2 kHz and 100 ms, respectively. Then the Doppler tolerances are approximately $d_r|_{\text{lfm}} \approx 0.3 \text{ B} \approx 36 \text{ kn}$ and $d_r|_{\text{bpsk}} \approx (1/T) \approx 0.6 \text{ kn}$. The latter is much smaller than the former. When $d_t = 1 \text{ kt}$, substitute them to (19), then $p_l|_{\text{lfm}} < 0.01$, $p_l|_{\text{bpsk}} = 0.99$. It means that for the same large BT LFM and BPSK waveforms, LFM has little clutter rejecting ability but BPSK is able to suppress almost all clutters when detecting a 1 kt target.

The received data are processed by multi-channel MF in Section 2, and the split-window normalisation is applied to envelope data to stabilise the reverberation data. When many clutters are presenting in the data, split-window normalisation tends to highlight the high-level returns and increase the SNR [1]. The ping-to-ping echograms of LFM and BPSK are shown in Fig. 5. Each subfigure shows the MF sequences of ten successive pings from bottom up. The four subfigures correspond to replica of Doppler shift (a) $d = 0 \text{ kt}$ for LFM, (b) $d = 1 \text{ kt}$ for LFM, (c) $d = 0 \text{ kt}$ for BPSK and (d) $d = 1 \text{ kt}$ for BPSK. As the sonar is moving towards the target, the target peak arriving moment is getting closer from ping 1 to ping 10. Similarly, the fixed clutters arriving moments are also getting closer to the sonar platform. The LFM outputs of replicas with Doppler shift 0 and 1 kt are almost the same except for a time delay which could be found by comparing Fig. 5a with Fig. 5b. Moreover, in Figs. 5c and d, it seems that the outputs of MF are quite different by using BPSK, the target is obvious in Fig. 5c by 1 kn replica and clutters are suppressed successfully. On the contrary, some clutters are clearly displayed in Fig. 5d with 0 kt replica and the target is suppressed. According to the relative distance of target and lighthouse, we can speculate that the biggest clutter which is called ‘clutter 2’ in Fig. 5d is formed by the lighthouse. The clutter 1 and others are all unknown underwater object echoes.

The above echograms cannot reflect the Doppler filter process sufficiently because only two Doppler replicas are used. Thus, only one ping data are chosen to be processed by using multi-replicas ranging from -2 to 2 kt , the results are shown in Fig. 6 which is named as ‘multi-Doppler gram’. The peak values of target and clutters are almost the same when LFM is adopted, but BPSK could separate target and clutters successfully because of the Doppler filter effect. For a more explicit comparison, the maximum values of target peak and clutter 2 peak are found out in Figs. 6a and b. Then the authors plot the peak values curve at each Doppler shift of LFM and BPSK in Fig. 7. Values are normalised to unity by the maximum value of each line. The peak value does not change much by LFM, however, the Doppler filter effect is obvious as shown in Fig. 7b. As the target velocity gets smaller or Doppler tolerance gets larger, the clutter reduction level degrades and is harder to separate the target from clutters. The name of ‘clutter filter’ could be understood clearly through the figure. If the minimum confidence probability $p_l = 0.95$ is required, according to (24), $I = 0.50 \text{ kt}$. From (23), it is required that $|\Delta d_t| - (d_t/2) > 0.5$. As $\Delta d_t = 1 \text{ kt}$, and then d_t have to be smaller than 1 kt. The BPSK satisfies this condition in our experiments. Thus, BPSK has a probability larger than 95% to reject clutters.

Through above analysis, when the authors choose and design the waveform according to the Doppler-statistic method, the clutter rejecting performance is fairly good. The clutter suppressing probability of BPSK in our experiments reaches as high as 99%. However, it is hard to figure out exactly how many of the clutters could be reduced. Thus, the authors employ the envelope-statistic method to verify and evaluate the problem.

As the sampling rate is equal to the transmit waveform bandwidth, consecutive samples are approximately uncorrelated. Thus, the data should be decimated by the rate of f_s/B , where f_s is the sample rate [5]. The data of each window (2048 samples) are tested by Mann-Whitney test to verify that they are identically distributed [11]. The data which failed to pass the test should be excluded. The other data are grouped as the estimation statistics. The data of BPSK and LFM are fitted by KD and the shape parameter α is estimated at different replica Doppler shifts varying from -5 to 5 kt separately. Verified by the KS test, the data are well fitted by KD and the estimated α curve with different replicas is shown in Fig. 8. In the figure, assuming $\hat{\alpha} = 20$ if $\hat{\alpha} > 20$, which represents $\hat{\alpha} \rightarrow \infty$ and KD turns to be Rayleigh model. As the figure shows, there is a minimum value that $\hat{\alpha}_{\text{BPSK}} \approx 6.2$ around Doppler range 0 kt. When replica Doppler shift deviates from 0 kt, $\hat{\alpha}_{\text{BPSK}}$ will increase quickly to be larger than 20. It’s because the BPSK’s Doppler tolerance is quite small and the Doppler spread of clutters is distributed around 0 kn corresponding to Fig. 3. In this case, as $\Delta d_t = 1 \text{ kt}$, almost all clutters have been rejected. However,

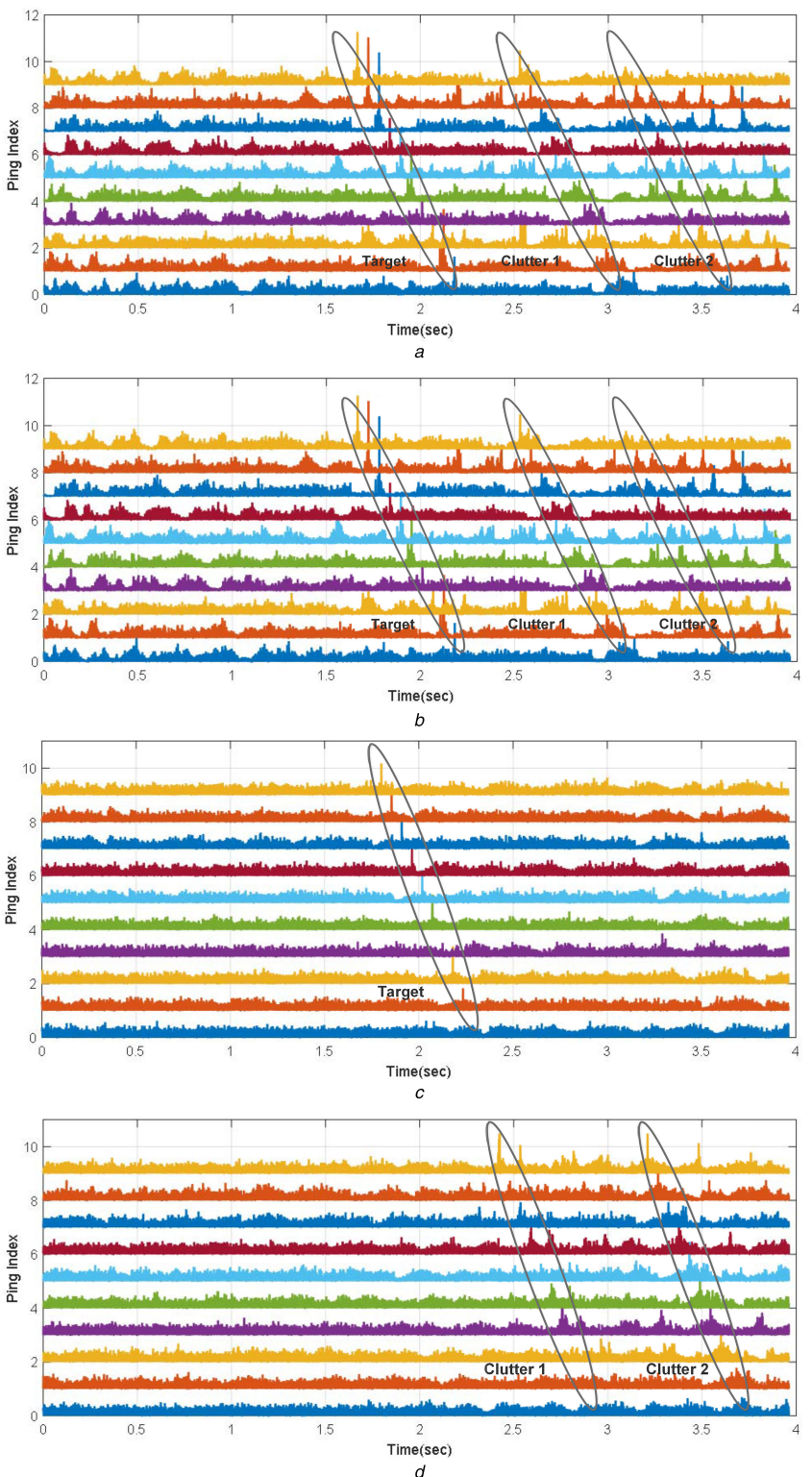


Fig. 5 Echogram comparison of LFM and BPSK experiments with different replicas

- (a) Echogram of LFM experiment with replica of Doppler 1 kt,
- (b) Echogram of LFM experiment with replica of Doppler 0 kt,
- (c) Echogram of BPSK experiment with replica of Doppler 1 kt,
- (d) Echogram of BPSK experiment with replica of Doppler 0 kt

$\hat{\alpha}_{\text{LFM}} \approx 2.6$ and maintains unchanged in a wide Doppler range. As $\hat{\alpha}_{\text{LFM}} < \hat{\alpha}_{\text{BPSK}}$, it means that the clutters suppressing performance of LFM is obviously worse than BPSK. Hence, the statistical parameters of envelope data are able to verify and compare the clutter rejecting performance successfully.

According to the above analysis, it is proved that the two methods are effective and feasible. We can calculate the probability of rejecting clutters theoretically in the Doppler-statistic method based on the reverberation Doppler spread model. It can be used as

a criterion to select and design waveforms for reducing clutters. The envelope-statistic method utilises the statistical parameters of envelope data to quantify the clutters in reverberation. It can be used to compare and verify the clutter rejecting performance of waveforms. Both the two methods are adopted on the basis of reverberation statistical features. Even though the hydrologic environment may be much more complex, and the models are difficult to be estimated accurately, the proposed methods provide novel ideas on the clutter rejecting problem from a new statistical

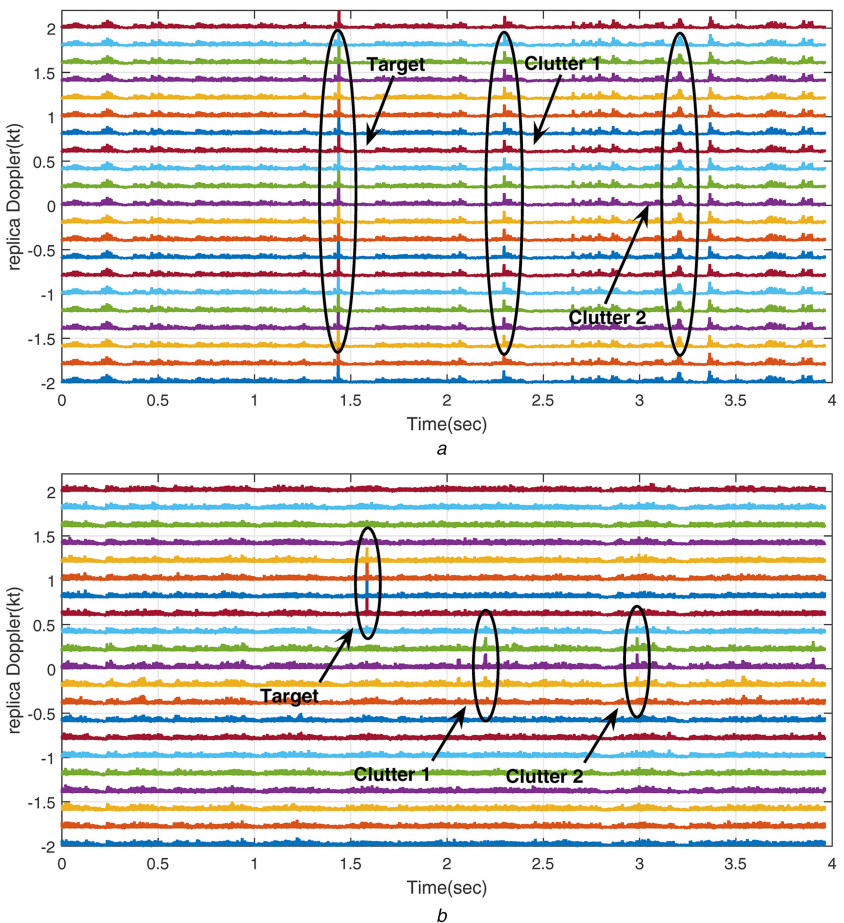


Fig. 6 Multi-Doppler MF gram with replicas Doppler from -2 to 2 kt for one ping

- (a) Multi-Doppler gram of LFM,
- (b) Multi-Doppler gram of BPSK

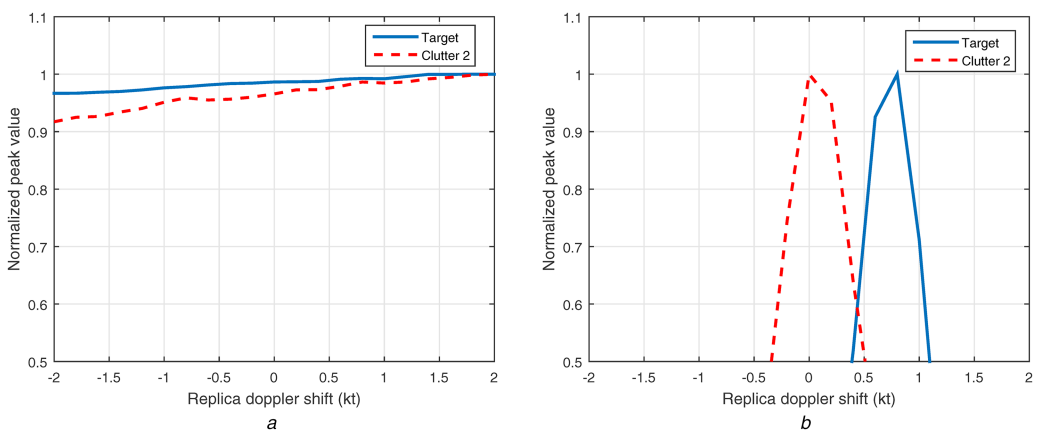


Fig. 7 Target and clutter 2 peak values curves with replica Doppler shift ranging from -2 to 2 kt by using LFM and BPSK

- (a) Target and clutter 2 peak values curves by using LFM,
- (b) Target and clutter 2 peak values curves by using BPSK

perspective. They are useful for sonar designer to improve the detection performance in clutter-filled environment.

5 Conclusion

This paper presents two methods, Doppler-statistic method and envelope-statistic method, separately, to estimate clutter suppressing performance of waveforms based on reverberation statistical features. The traditional evaluation methods of waveforms are commonly based on waveform parameters, which do not take environmental factors into account. In order to reduce clutters and false alarms, it is not suitable to blindly design waveforms without considering the variation of clutters. In this paper, two methods are statistically proposed to calculate the

probability of rejecting clutters and verify clutter suppressing performance of waveforms. The methods are feasible and helpful for sonar designers to reduce false alarms and improve detection performance.

6 Acknowledgments

This work was partly supported by the National Natural Science Foundation of China (NSFC) under the project grant nos. 61471352, 61671443, 61302169, 61531018 and 61372181.

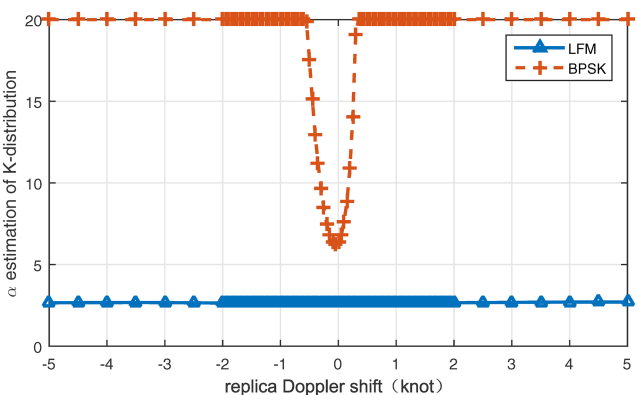


Fig. 8 Estimated α of LFM and BPSK by different replicas of Doppler shifts ranging from -10 to 10 kt. Doppler spread of clutters contribute to the smaller α around Doppler shift 0 kn of BPSK curve

7 References

- [1] Yang, T.C., Schindall, J., Huang, C.F., *et al.*: ‘Clutter reduction using Doppler sonar in a harbor environment’, *J. Acoust. Soc. Am.*, 2012, **132**, 5, pp. 3053–3067
- [2] Colin, M.E.G.D., Beerens, S.P.: ‘False-alarm reduction for low-frequency active sonar with BPSK pulses: experimental results’, *IEEE J. Ocean. Eng.*, 2011, **36**, 1, pp. 52–59
- [3] Prior, M.K., Baldacci, A.: ‘The physical causes of clutter and its suppression via sub-band processing’, *Conf. Oceans IEEE*, 2006, pp. 1–6
- [4] Abraham, D.A., Gelb, J.M., Oldag, A.W.: ‘Background and clutter mixture distributions for active sonar statistics’, *IEEE J. Ocean. Eng.*, 2011, **36**, 2, pp. 231–247
- [5] Abraham, D.A., Lyons, A.P.: ‘Novel physical interpretations of K-distributed reverberation’, *IEEE J. Ocean. Eng.*, 2002, **27**, 4, pp. 800–813
- [6] van Walree, P.A., Jenserud, T., Smedsrød, M.: ‘A discrete-Time channel simulator driven by measured scattering functions’, *IEEE J. Sel. Areas Commun.*, 2009, **26**, 9, pp. 1628–1637
- [7] Murray, J.J.: ‘A theoretical model of linearly filtered reverberation for pulsed active sonar in shallow water’, *J. Acoust. Soc. Am.*, 2014, **136**, 5, pp. 2523–2531
- [8] Gelb, J.M., Heath, R.E., Tipple, G.L.: ‘Statistics of distinct clutter classes in midfrequency active sonar’, *IEEE J. Ocean. Eng.*, 2010, **35**, 2, pp. 220–229
- [9] Abraham, D.A., Lyons, A.P.: ‘Simulation of non-Rayleigh reverberation and clutter’, *IEEE J. Ocean. Eng.*, 2004, **29**, 2, pp. 347–362
- [10] Abraham, D.A., Lyons, A.P.: ‘Reverberation envelope statistics and their dependence on sonar bandwidth and scattering patch size’, *Ocean. Eng. IEEE J.*, 2004, **29**, 1, pp. 126–137
- [11] Lyons, A.P., Abraham, D.A.: ‘Statistical characterization of high-frequency shallow-water seafloor backscatter’, *J. Acoust. Soc. Am.*, 1999, **106**, 3, pp. 1307–1315
- [12] Etter, P.C.: ‘Underwater acoustic modeling and simulation’ (CRC Press, 2013, 4th edn.), pp. 291–309

- [13] Rihaczek, A.W.: 'Delay-Doppler ambiguity function for wideband signals', *IEEE Trans. Aerosp. Electron. Syst.*, 1967, **3**, 4, pp. 705–711
- [14] Jourdain, G., Henrioux, J.P.: 'Use of large bandwidth duration binary phase shift keying signals in target delay Doppler measurements', *J. Acoust. Soc. Am.*, 1991, **90**, 1, pp. 299–309
- [15] Mours, A., Mars, J.I., Ioana, C., et al.: 'Range, velocity and immersion estimation of a moving target in a water-filled tank with an active sonar system', *Conf. Oceans IEEE*, 2015, pp. 1–6
- [16] Abraham, D.A., Lyons, A.P.: 'Reliable methods for estimating the K -distribution shape parameter', *IEEE J. Ocean. Eng.*, 2010, **35**, 2, pp. 288–302
- [17] Preston, J.R., Abraham, D.A.: 'Statistical analysis of multistatic echoes from a Shipwreck in the Malta plateau', *IEEE J. Ocean. Eng.*, 2014, **40**, 3, pp. 1–14
- [18] Collins, T., Atkins, P.: 'Doppler-sensitive active sonar pulse designs for reverberation processing', *IEE Proc.-Radar Sonar Navig.*, 1999, **145**, 6, pp. 347–353
- [19] Nakahira, K., Okuma, S., Kodama, T., et al.: 'The use of binary coded frequency shift keyed signals for multiple user sonar ranging'. IEEE Int. Conf. Networking, 2004, vol. 2, pp. 1271–1275
- [20] Yang, T.C., Yang, W.B.: 'Interference suppression for code-division multiple-access communications in an underwater acoustic channel', *J. Acoust. Soc. Am.*, 2009, **126**, 1, pp. 220–228